VNU Journal of Science: Mathematics – Physics, Vol. 33, No. 3 (2017) 25-29

First-principles Calculations on Electronic Properties of $LaNiO_3$ in Solid Oxide Fuel Cell Cathodes

Pham Ba Duy*, Nguyen Duy Huy, Bach Thanh Cong

Computational Materials Science Laboratory,
Faculty of Physics, VNU University of Science, 334 Nguyen Trai, Hanoi, Vietnam

Received 09 August 2017
Revised 30 August 2017; Accepted 19 September 2017

Abstract: First-principles calculations based on the density functional theory are used to study the electronic structure of $LaNiO_3$ perovskite for application of cathode material in solid oxide fuel cell. Our results show that bulk $LaNiO_3$ exhibits metallic behavior. For 1x1x1 $LaNiO_3$ unit cell, increasing in-plane strain leads to the increase in the density of states (DOS) at the Fermi level. On the other hand, the DOS at the Fermi level for 2x2x2 $LaNiO_3$ supercell first increases with the strain up to 3% and then decreases for larger values of the strain. The difference between the electronic structure of the 2x2x2 supercell and that of the 1x1x1 unit cell is attributed to the rotations of NiO_6 octahedra.

Keywords: Solid oxide fuel cell, density functional theory, $LaNiO_3$ perovskite, electronic structures, strain.

1. Introduction

The perovskite $LaNiO_3$ is frequently used as cathode material for solid oxide fuel cells due to its high temperature stability, acceptable thermal expansion, and the ability to enhance oxygen reduction reaction [1-4]. At cathode-electrolyte interface, the induced strain caused by lattice mismatch between $LaNiO_3$ and electrolyte materials is expected to give rise to the reconstructions of the electronic structures of $LaNiO_3$. Such electronic reconstructions could be important as they are tightly linked with the formation of oxygen vacancy and the conduction of oxygen ions, which greatly affect the operation of the fuel cell. On the other hand, previous publications have reported that the NiO_6 octahedra rotated in bulk $LaNiO_3$, alternating the electronic structure [5, 6]. As a result of the induced strain at the cathode-electrolyte interface, such octahedral rotations can be enhanced or suppressed. In this paper, we investigate the electronic structure and NiO_6 octahedral rotations of $LaNiO_3$ under epitaxial strain using first-principles calculations.

*Corresponding author. Tel.: 84-915054648.
Email: duy.pham.ba@gmail.com
https//doi.org/ 10.25073/2588-1124/vnumap.4218

2. Computational details

All calculations are performed based on the density functional theory [7] using plane-wave basis sets [8] as implemented in the Quantum Espresso package [9]. The exchange-correlation interaction is treated using local density approximation (LDA) with the Perdew-Zunger parametrization [10], and the electron-ion interaction is described by Vandebilt ultrasoft pseudopotentials [11].

The computational models of 1x1x1 unit cell and 2x2x2 supercell of $LaNiO_3$ are shown in Fig. 1. Periodic boundary conditions are imposed in all dimensions. The kinetic energy cutoff for wavefunctions is chosen at 680 eV and sufficient k-point sampling is employed in the Brillouin zone. Structural optimizations are performed until all remaining forces acting on each atom are less than 0.03 eV/Å.

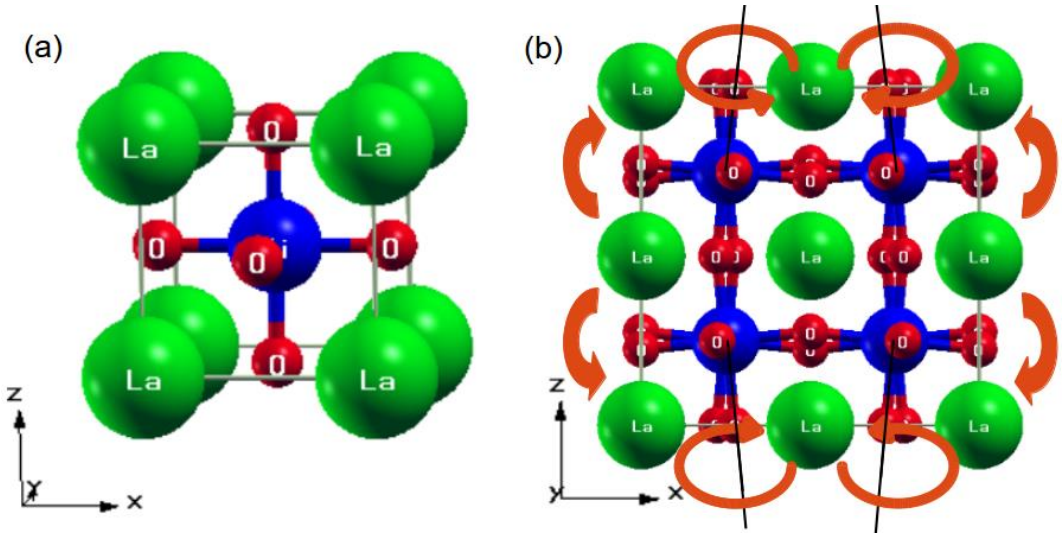

Fig. 1. Computational models of (a) 1x1x1 $LaNiO_3$ unit cell and (b) 2x2x2 $LaNiO_3$ supercell without in-plane strain, indicating rotations of NiO_6 octalhedra. The small red, big green, and medium blue balls indicate O, La, and Ni atoms, respectively. The rectangular boxes represent supercells.

Previous experimental publication has reported that the epitaxial strain at the interface of $LaNiO_3$ layers and the substrate penetrates deep into the $LaNiO_3$ inner layers [12]. Thus, it is assumed that the imposed strain throughout our models is uniform. To simulate the strained $LaNiO_3$ layers, we fix the in-plane lattice parameters and allow the out-of-plane lattice parameter of the 1x1x1 unit cell to relax. We choose various in-plane strains from -3% to 5% as observed in experiments [13, 14]. Then, the 2x2x2 $LaNiO_3$ supercell is constructed (by doubling the obtained lattice parameters of the 1x1x1 unit cell), allowing for local rotations of NiO_6 octahedra.

3. Results and discussion

The optimized lattice parameters of the 1x1x1 $LaNiO_3$ unit cell are found to be $l_{cal}=l_x=l_y=l_z=$ 3.749 Å, which are 2.3% smaller than the published experimental data [3]. The underestimation of the lattice parameters is typical of LDA calculations [15, 16].

Figure 2 shows the out-of-plane strain $u_z = l_z/l_{cal} - 1$ as a function of the in-plane strain $u_{xy} = l_x/l_{cal} - 1$ for the 1x1x1 $LaNiO_3$ unit cell, where l_x and l_z are the in-plane and out-of-plane lattice parameters,

respectively, and l_{cal} is the non-strained equilibrium one. It can be seen that u_z declines (almost linearly) by 0.6% for each 1.0% increase in u_{xy}. The computed out-of plane strain of $LaNiO_3$ on $SrTiO_3$ substrate is found to be 1.0% as compared to the experimental value of 0.7% [5].

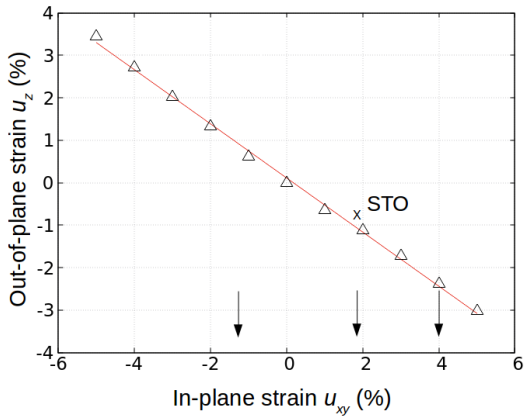

Fig. 2. Calculated out-of-plane strain u_z vs in-plane strain u_{xy}. x: experimental value for a $LaNiO_3$ film grown on $SrTiO_3$ substrate. Vertical arrows designate in-plane strains of commercially available substrates, from left to right: $LaAlO_3$, $SrTiO_3$, and $KTaO_3$.

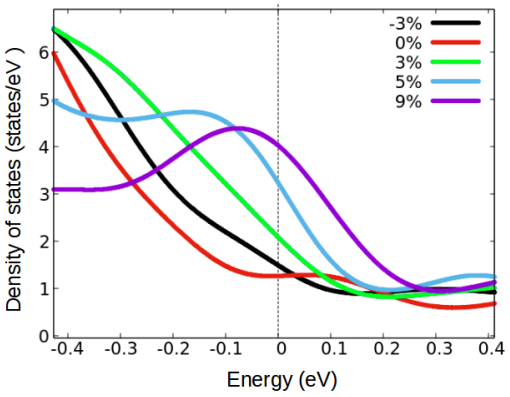

Fig. 3. Total DOS of 1x1x1 $LaNiO_3$ unit cell for various values of in-plane strain u_{xy}. The Fermi level is chosen at 0 eV.

Figure 3 presents the total DOS of 1x1x1 $LaNiO_3$ unit cell for various in-plane strains. As one can see, $LaNiO_3$ keeps the metallic behavior, and the total DOS near the Fermi level is enhanced with the strain. Specifically, the DOS is increased by 2.7 times as u_{xy} increases from -2% to 5%. Previous publications have shown that states near the Fermi level of bulk $LaNiO_3$ are formed by the hybridization between Ni 3*d* and O 2*p* orbitals [2, 17-19]. Thus, we plot in Fig. 4 the projected DOS of strained $LaNiO_3$ onto Ni t_{2g} and e_g orbitals. For the non-strained case, t_{2g}-derived states are completely filled, and the e_g-derived states are occupied by one electron. For $u_{xy} > 0\%$, t_{2g}-derived states become partially occupied as a result of the changes in Ni-O bond distances. In the vicinity of the Fermi level, the density of t_{2g}-derived states increases with increasing u_{xy}, whereas that of e_g-derived states first increases and then decreases as u_{xy} is larger than 3%. As the changes in the density of t_{2g}-derived states are substantial compared to those of e_g-derived states, the total DOS at the Fermi level increases with the in-plane strain.

For the 2x2x2 $LaNiO_3$ supercell, the electronic structure is expected to deviate from that of the 1x1x1 unit cell. The rotations of NiO_6 octahedra inside the supercell change the Ni-O-Ni bonding angles (see Fig. 1(b)) and thus alter the hybridization between Ni 3*d* and O 2*p* orbitals. Figure 5 indicates the dependence of Ni-O-Ni angles along the *z* direction (α_z) and in the *xy* plane (α_{xy}) on the in-plane strain. It is noted that the in-plane strain in the case of 2x2x2 supercell is the same as that in 1x1x1 unit cell. By increasing u_{xy}, α_z (α_{xy}) decreases (increases), implying the reduction (enhancement) of the *p-d* hybridization. Thus, a competition in the contributions of *p-d* hybridized states along the *z* direction and in the *xy* plane to the electronic structure is expected. We plot in Fig. 6 total DOS of the 2x2x2 $LaNiO_3$ supercell with respect to the in-plane strain. In contrast to the 1x1x1 unit cell case, where the DOS at the Fermi level increases with increasing u_{xy} (see Fig. 3), the DOS at the Fermi level of the 2x2x2 supercell first increases with u_{xy} up to 3% and then decreases. This behavior can be attributed to the rotations of NiO_6 octahedra, which alters the electronic structure in the vicinity of the Fermi level.

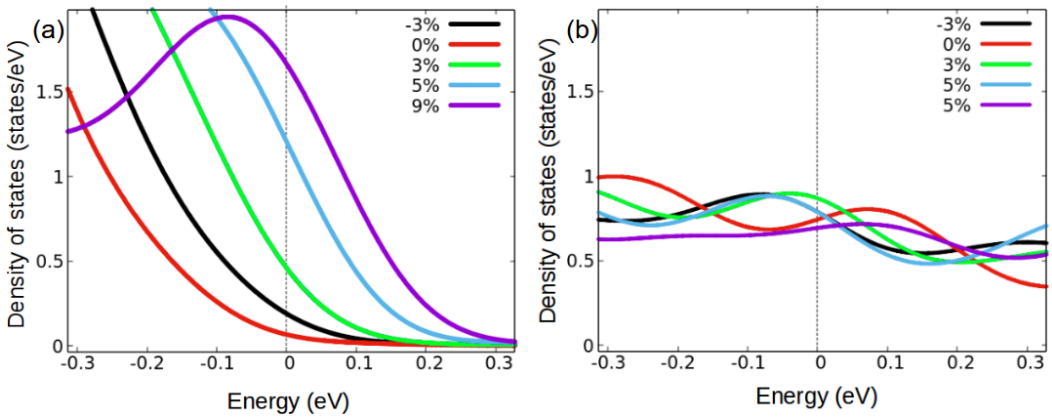

Fig. 4. Projected DOS of 1x1x1 $LaNiO_3$ unit cell onto (a) t_{2g} and (b) e_g orbitals of Ni atom for various values of in-plane strain u_{xy}. The Fermi level is chosen at 0 eV.

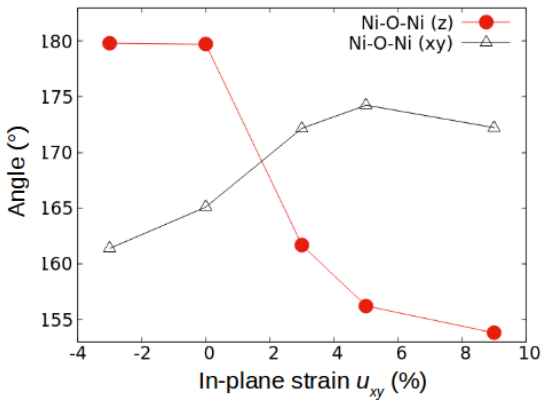

Fig. 5. Ni-O-Ni angles along *z* direction (red line) and in *xy* plane (black line) as functions of the in-plane strain u_{xy}.

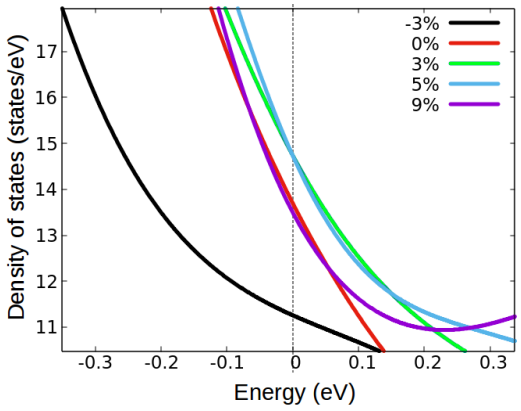

Fig. 6. Total DOS of 2x2x2 $LaNiO_3$ supercell for various values of in-plane strain u_{xy}. The Fermi level is chosen at 0 eV.

4. Conclusions

First-principles calculations are employed to investigate the electronic structure of bulk $LaNiO_3$ under epitaxial strain. By applying strain, the Ni t_{2g}-derived states of the 1x1x1 unit cell become partially occupied. In the vicinity of the Fermi level, the density of the t_{2g}-derived states increases with u_{xy} while that of the e_g-derived states increases for u_{xy} < 3% and then decreases for larger u_{xy}. In addition, the variation of density of the t_{2g}-derived states is much larger than that of the e_g-derived states, resulting in the increase of the total DOS at the Fermi level with respect to the in-plane strain. For the 2x2x2 $LaNiO_3$ supercell, rotations of the NiO_6 octahedra are observed, altering the *p-d* hybridization. The total DOS at the Fermi level first increases for values of the in-plane strain lower than 3% and then decreases for larger strain. Our results are the first step towards further calculations regarding oxygen-defected $LaNiO_3$ systems and migration paths of oxygen ions.

Acknowledgements

This research is funded by the Vietnam National University, Hanoi (VNU) under project number QG.17.10.

References

[1] S. B. Adler, "Factors governing oxygen reduction in solid oxide fuel cell cathodes", Chem. Rev. 104, 4791 (2004).

[2] M. L. Medarde, "Structural, magnetic and electronic properties of $RNiO_3$ perovskites (R = rare earth)", J. Phys.: Condens. Matter 9, 1679 (1997).

[3] J.-S. Zhou, J. B. Goodenough, B. Dabrowski, P. W. Klamut, and Z. Bukowski, "Enhanced susceptibility in $LNiO_3$ perovskites (L=La,Pr,Nd,$Nd_{0.5}$ $Sm_{0.5}$)", Phys. Rev. Lett. 84, 526 (2000).

[4] J. B. Torrance, P. Lacorre, A. I. Nazzal, E. J. Ansaldo, and Ch. Niedermayer, "Systematic study of insulator-metal transitions in perovskites $RNiO_3$ (R=Pr,Nd,Sm,Eu) due to closing of charge-transfer gap", Phys. Rev. B 45, 8209(R) (1992).

[5] J. L. García-Muñoz, J. Rodríguez-Carvajal, P. Lacorre, and J. B. Torrance, "Neutron-diffraction study of $RNiO_3$ (R=La,Pr,Nd,Sm): Electronically induced structural changes across the metal-insulator transition", Phys. Rev. B 46, 4414 (1992).

[6] S. J. May, J.-W. Kim, J. M. Rondinelli, E. Karapetrova, N. A. Spaldin, A. Bhattacharya, and P. J. Ryan, "Quantifying octahedral rotations in strained perovskite oxide films", Phys. Rev. B 82, 014110 (2010).

[7] A. E. Mattsson, P. A. Schultz, M. P. Desjarlais, T. R. Mattsson, and K. Leung, "Designing meaningful density functional theory calculations in materials science-a primer", Modell. Simul. Mater. Sci. Eng. 13, R1 (2005).

[8] G. Kresse and J. Furthmüller, "Efficiency of ab-initio total energy calculations for metals and semiconductors using a plane-wave basis set", Comp. Mater. Sci. 6, 15 (1996).

[9] P. Giannozzi et al., "QUANTUM ESPRESSO: a modular and open-source software project for quantum simulations of materials.", J. Phys.: Condens. Matter 21, 395502 (2009).

[10] J. P. Perdew and A. Zunger, "Self-interaction correction to density-functional approximations for many-electron systems", Phys. Rev. B 23, 5048 (1981).

[11] K. Laasonen, R. Car, C. Lee, and D. Vanderbilt, "Implementation of ultrasoft pseudopotentials in ab initio molecular dynamics", Phys. Rev. B 43, 6796 (1991).

[12] A. Yu. Dobin, K. R. Nikolaev, I. N. Krivorotov, R. M. Wentzcovitch, E. Dan Dahlberg, and A. M. Goldman, "Electronic and crystal structure of fully strained $LaNiO_3$ films", Phys. Rev. B 68, 113408 (2003).

[13] J. Zhu, L. Zheng, Y. Zhang, X. H. Wei, W. B. Luo, and Y. R. Li, "Fabrication of epitaxial conductive $LaNiO_3$ films on different substrates by pulsed laser ablation", Mater. Chem. Phys. 100, 451 (2006).

[14] J. Yu, X. J. Meng, J. L. Sun, Z. M. Huang, and J. H. Chu, "Optical and electrical properties of highly (100)-oriented $PbZr_{1-x}Ti_xO_3$ thin films on the $LaNiO_3$ buffer layer", J. Appl. Phys. 96, 2792 (2004).

[15] A. van de Walle and G. Ceder, "Correcting overbinding in local-density-approximation calculations", Phys. Rev. B 59, 14992 (1999).

[16] P. Haas, F. Tran, and P. Blaha, "Calculation of the lattice constant of solids with semilocal functionals", Phys. Rev. B 79, 085104 (2009).

[17] Š. Masys, S. Mickevičius, S. Grebinskij, and V. Jonauskas, "Electronic structure of $LaNiO_{3-x}$ thin films studied by X-ray photoelectron spectroscopy and density functional theory", Phys. Rev. B 82, 165120 (2010).

[18] L. Guan, B. Liu, L. Jin, J. Guo, Q. Zhao, Y. Wang, G. Fu, "Electronic structure and optical properties of $LaNiO_3$: First-principles calculations", Solid State Commun., 150, 2011 (2010).

[19] K. P. Rajeev, G. V. Shivashankar, A. K. Raychaudhuri, "Low-temperature electronic properties of a normal conducting perovskite oxide ($LaNiO_3$)", Solid State Commun., 79, 591 (1991).